First Paleomagnetic Record of the Matuyama-Brunhes Transition in the Loess-Paleosol Series of Tajikistan

Ekaterina Kulakova and Redzhep Kurbanov

Abstract Detailed paleomagnetic records of the Matuyama-Brunhes (M/B) magnetic polarity transition in continuous sedimentary sequences both provide a geochronological constraint on the sequence and expand our knowledge of the reversal process. Although the age of the Matuyama-Brunhes reversal has been studied in detail, some high-resolution geological archives show a discrepancy in the actual and expected position of the M/B boundary, e. g. loess-paleosol sequences of Central Asia and China. We have carried out a detailed paleomagnetic study of the M/B transition in the loess-paleosol sequence at the Kuldara site, Tajikistan, the first such study in the region. Matuyama-Brunhes transition at the Kuldara site encompasses 3 m thick zone, and includes 7 polarity flips and zones with anomalous directions. The transition zone begins in the MIS 20 loess and ends in the lowermost part of the MIS 19 warm stage. Preliminary duration estimate for the transition is ~22 kyr, and its lower and upper limits have older ages than expected (809–787 ka). However, the last reliable zone of reverse polarity is found at the beginning of MIS 19, reported for the first time for this loess-paleosol section. Furthermore, we have found an excursion (852–847 ka) ~38 kyr prior to the reversal which manifests itself as a 22 cm thick zone with anomalous directions and instable paleomagnetic signal. Nevertheless, the magnetic reversal event appears somewhat older compared to other sedimentary and volcanic records of the M/B transition. Delayed acquisition or superimposed younger magnetization in the studied loesses may be the reason for this discrepancy, and requires further study.

E. Kulakova (✉)
Schmidt Institute of Physics of the Earth RAS, B. Gruzinskaya 10, 123242 Moscow, Russia
e-mail: ek.kula@yandex.ru

E. Kulakova · R. Kurbanov
Institute of Archaeology and Ethnography SB RAS, Acad. Lavrentiev Avenue 17, 630090 Novosibirsk, Russia

R. Kurbanov
Lomonosov Moscow State University, Leninskie Gory 1, 119991 Moscow, Russia

Institute of Geography RAS, Staromonetniy Lane 29, 119017 Moscow, Russia

A. Kosterov et al. (eds.), *Problems of Geocosmos—2022*, Springer Proceedings in Earth and Environmental Sciences, https://doi.org/10.1007/978-3-031-40728-4_6

Keywords Matuyama-Brunhes polarity transition · Loess-paleosol series · Paleomagnetism

1 Introduction

The last geomagnetic reversal, the Matuyama-Brunhes (M/B) polarity transition, is a significant stratigraphic and geochronological marker for calibrating the age of Quaternary sedimentary sequences. Despite a long history of studies, mechanisms of magnetic field reversal, its configuration and timing still remain controversial and insufficiently understood [1, 2]. When a sedimentary sequence is continuous, has sufficient thickness and is able to capture the magnetic signal without a long delay, it may allow a deeper look at the behavior of the magnetic field itself. This explains an interest in detailed studies of the M/B boundary transition zone in various sediments.

The loess-paleosol series are unique continental archives of geological information. This type of deposits is sensitive to climatic fluctuations of the Quaternary period, when strong winds prevailed during the cold stages of the climate bring dust from nearby deserts and deposit thick loess strata [3, 4]. Within loess sequence, soils are formed during interglacials with increasing humidity and global temperature [5]. Central Asian and Chinese losses are considered to be the most complete record of dust sedimentation and well-correlated with various climatic proxies, primarily, with marine isotope stages (MIS) using a magnetic susceptibility [6]. This leads to the expected M/B boundary position in the paleosol corresponding to MIS 19, as found in marine sediments [7]. However, paleomagnetic data for the most Chinese, Central Asian and some European loess sections place the M/B boundary in the loess layer of MIS 20 [8–10], at odds with the marine data. An independent method for determining the Matuyama-Brunhes boundary position based on meteoric ^{10}Be gives a result consistent with marine sediments, indicating a problem of magnetic overprinting of primary magnetization in Asian loesses [11].

Many well-studied reference loess-paleosol sections of Tajikistan (Central Asia) (Table 1) contain a record of the Matuyama-Brunhes polarity transition which is found in the loess layer between pedocomplexes 10 and 9 [12], corresponding to MIS 21 and 19, respectively [9]. Pedocomplex (PC) is a traditional stratigraphic unit, which usually consist of several combined soils of the same interglacial. Only in rare cases M/B boundary was found at the base of PC 9, e.g. in Karamaidan section [13] and Darai Kalon [14]. In most cases, M/B position is at odds with the marine sediment data, as emphasized above. However, Tajik loesses were never subjected to the detailed high-resolution paleomagnetic investigation and, therefore, require such study to refine their chronostratigraphy and carry out interregional correlations.

Table 1 Reference loess-paleosol sections of Tajikistan [after [4, 15, 16], and recent field work of authors]

Section name	Location	Thickness (m)	Number of PCs	Archaeological significance
Chashmanigar/ Darai Kalon	38°23′25.87″ N 69°49′ 58.33″ E	215 / 176	29 / 18	PC5
Kaiburak	~38°25′3.50″ N 69°44′34.91″ E	120	13	PC4
Karamaidan	~38°34′52.57″ N 69°14′4.91″ E	100 (up to 200)	13 (up to 47)	PC6
Karatau	~38°23′19.92″ N 69°10′6.53″ E	95	7	PC6 (PC5)
Khonako-II	38°21′33.38″ N 70° 2′46.99″ E	120	16	PC4–PC1, mostly in PC2
Kuldara	38°16′57.97″ N 69°53′8.30″ E	115	15	PC12–PC11
Obi-Mazar/ Lakhuti	38°18′08.90″ N 69°53′29.73″ E	80	7	PC6–PC4, mostly in PC5
Tagijar	~38°17′51.84″ N 69°54′41.75″ E	145	17	PC5, PC4

2 Geological Setting and Methods

2.1 Object of the Study

Loess-paleosol sequences are widespread in southern Tajikistan covering vast areas of the Pamir piedmont (Fig. 1) and having an age up to 2.6 million years [15]. Furthermore, Tajik loess-paleosol sequences have an archaeological significance, containing stone tool industries of different age united under the term «Loessic Paleolithic» [16].

Kuldara site (N 38.28277°, E 69.88564°) is the earliest known archaeological site in the region with stone artefacts found in pedocomplexes 11 and 12 (MIS 23-25) [16]. Since magnetostratigraphy is a basis for the chronological constrains of the Kuldara site, an accurate paleomagnetic chart is important for age estimations of the initial hominin dispersal to the region. In 2021, we revisited the section, where the fieldwork was last carried out in the 1980s, to study it with new methods and at the modern level of quality and reliability.

The Kuldara section is 84 m thick and reveals a stratigraphic sequence from the Holocene soil to PC 11 (Fig. 1c); however, it has a hiatus at the upper part which is expressed in the absence of PC 3. Pedocomplexes in Tajikistan are often underlied by petrocalcic horizons which are thick and hard calcic-cemented horizons of illuvial origin, formed during the period of the soil climatic optimum. The layers have a dip (azimuth 57, angle 13) which is almost the same for the entire section. This

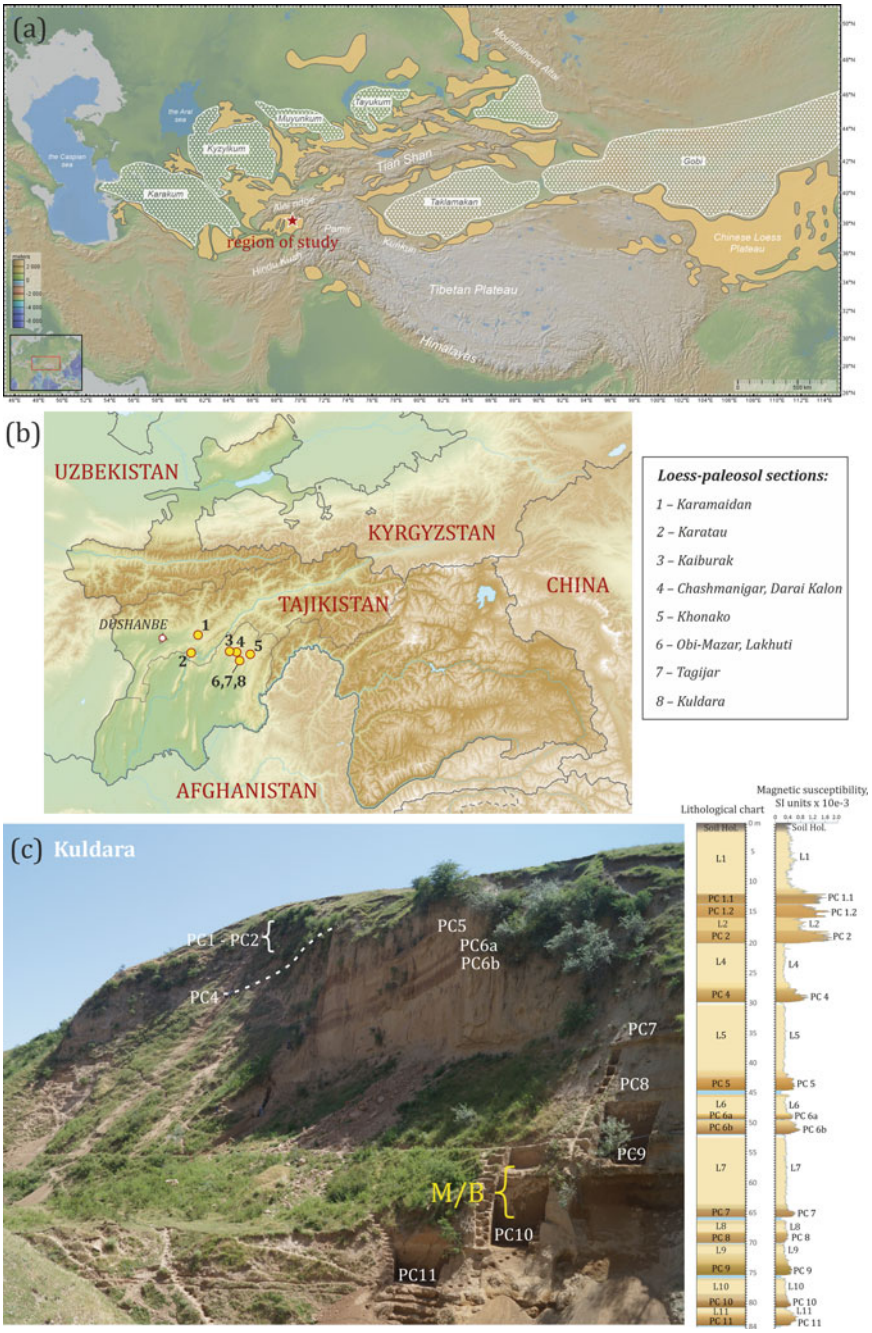

Fig. 1 **a** location of the study site on the loess distribution map. **b** location of the Kuldara section with other previously studied sections of Tajik loess [15]. **c** general view on the Kuldara site with position of pedocomplexes and Matuyama-Brunhes (M/B) polarity transition, lithological chart, and magnetic susceptibility curve measured in the field. PC—pedocomplex, L—loess

is a slope direction of the paleorelief surface on which dust accumulated and soils developed in the past. Therefore, the geographic system of samples coincides with the stratigraphic one.

First, reconnaissance paleomagnetic sampling with a 50 cm resolution was done for the entire section in June 2021. It yielded a magnetostratigraphic polarity scale and determined an approximate position of the M/B transition. This interval was then, in September 2021, sampled continuously for a high-resolution paleomagnetic study.

2.2 Methods

Paleomagnetic studies

The ~3 m interval containing a record of the magnetic polarity transition determined by a low-resolution paleomagnetic study was expanded to cover stable polarity record above and below the transition zone and sampled continuously with paleomagnetic blocks. The blocks (each 10–20 cm high and ~10 cm wide) were cut from the section with a knife, oriented and then sampled. Orientation was performed by the standard technique, measuring dipping elements of the front sub-vertical side of block prepared as a plain surface. In total, a 5 m loess-paleosol interval covering the PC 9, loess L10, and PC 10 was sampled continuously to study the record of the M/B polarity transition (Fig. 2a). Oriented blocks were cut into ~2 cm thick horizontal slices using a rock-sawing machine in the laboratory (Fig. 2b, c). Samples from 230 horizontal (stratigraphic) levels have been collected. Every level was cut further into cubes, and 4–5 cube specimens from each level were obtained (Fig. 2d). The first 3 blocks (19 levels, depth 74.53–75.19 m) correspond to PC9. Next 50 cm of section below the PC9 is a petrocalcic horizon (75.19–75.73 m) where sampling was not possible. Petrocalcic horizons contain abundant carbonates leading to low magnetic susceptibility and magnetization values, and are challenging to sample without a rock sawing machine. Blocks 4–26 correspond to L10 (149 levels, 75.73–78.64 m), and blocks 27–34 correspond to PC10 (62 levels, 78.64–80 m). A total of 1460 specimens were prepared for paleomagnetic measurements.

Natural remanent magnetization (NRM) was measured using a 2G Enterprises cryogenic SQUID-magnetometer in a magnetically shielded room at the laboratory of Main Geomagnetic Field and Rock Magnetism of Schmidt Institute of Physics of the Earth RAS, Moscow. Two cubes from each stratigraphic level were subjected to progressive thermal demagnetization with 30–50° increment up to 580°. The rest sister specimens were subjected to progressive alternating field (AF) demagnetization with 5–10 mT increment up to 120 mT.

The characteristic component from each sample was identified by the principal component analysis [17]. The mean direction was calculated for each stratigraphic level using Fisher statistics [18], with obvious directional outliers and specimens with maximum angular deviation (MAD) >15° discarded. To indicate the quality of

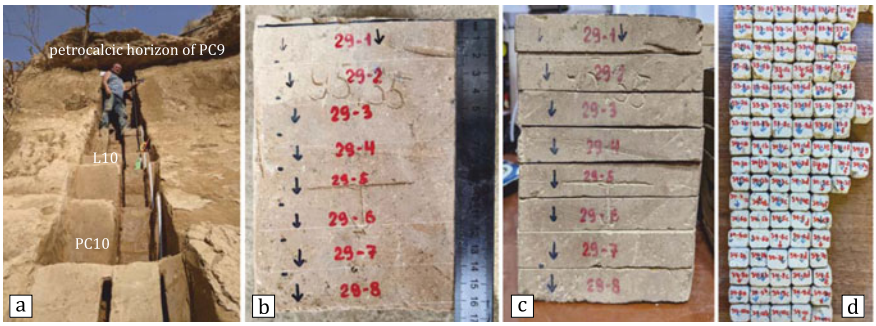

Fig. 2 Paleomagnetic sample collection and preparation. **a** continuous sampling of the oriented blocks from the trench. **b** oriented block prepared for sawing. **c** the same block sliced into 2-cm levels. **d** paleomagnetic cubic specimens (duplicates)

the record, we calculated the mean MAD value by arithmetically averaging MAD values of all specimens from the same level. Taking into account that the number of specimens for each stratigraphic level was different, the α_{95} parameter was not representative for this purpose.

Virtual geomagnetic poles (VGP) were calculated using the mean component directions at every level. Polarity interpretation is based on VGP latitude where VGP latitudes >45° were defined as normal polarity, latitudes < −45° as reversed polarity, and latitudes between −45° and 45° as intermediate/anomalous polarity, respectively.

Rock magnetic studies

The magnetic susceptibility measurements in the field were carried out continuously using a portable PIMV kappameter (Geodevice, Russia) for the entire thickness of the section with 3 cm resolution. Sensor area of the kappameter is 3 × 9 cm, sensitivity is 1×10^{-7} SI units.

For the studied transitional M/B interval, magnetic susceptibility and its frequency dependence were measured in the laboratory for one specimen from every level. Measurements of bulk magnetic susceptibility were made for two frequencies (976 Hz and 15,616 Hz) with a Kappabridge MFK1-FA (AGICO) instrument. All measurements are normalized by mass. Frequency dependence, χ_{fd}, is defined as follows: $\chi_{fd}\,(\%) = (\chi_{976Hz} - \chi_{15616Hz})/\chi_{976Hz} \times 100$.

To determine the magnetic mineralogy, additional rock magnetic investigations were carried out on a few selected samples from pedocomplexes 9, 10, and loess 10. Hysteresis loops, IRM acquisition and backfield demagnetization curves were measured using a PMC MicroMag 3900 Vibrating Sample Magnetometer in the maximum field 1.8 T. Anisotropy of magnetic susceptibility (AMS) was measured using a Kappabridge MFK1-FA instrument. Temperature dependence of magnetic susceptibility was traced using a Kappabridge MFK1-FA connected with a CS3 high-temperature furnace. Powdered samples were heated in air from room temperature to 700 °C with a heating rate of ~13.7 °C/min and then cooled back to room temperature.

3 Results

3.1 Magnetic Mineralogy

Hysteresis loops show slight differences in magnetic coercivity (B_c) and loop shape (Fig. 3) for soil samples from PC9 and PC10 and loess sample from L10. Although the loops close only at ~800 mT (Fig. 3) and IRM acquisition curves do not reach saturation by 1.8 T, soft magnetic minerals (e.g., magnetite, maghemite) appear to dominate the magnetic signal. As shown in the example in Fig. 3, and true for the entire section, all loess samples have higher coercivity than soil samples. Loess has higher relative content of hematite as well as coarser size of detrital magnetite in comparison with magnetite of pedogenic origin in soils. Ultrafine grain size of pedogenic magnetic minerals is confirmed by frequency dependence of magnetic susceptibility (Fig. 4) [19], where increased values of χ_{fd} are observed in LB in the topmost part of PC 10 and in soil layers affected by pedogenesis. For soil samples from PC 9 and PC 10 S-ratio$_{(100\ mT)}$ is 0.37 and 0.36, respectively, for loess sample from L 10 S-ratio$_{(100\ mT)} = 0.31$. S-ratio$_{(300\ mT)}$ is about 0.83 for both soil and loess samples, indicating a coarser size of soft-magnetic fraction in loess.

Thermomagnetic analysis of magnetic susceptibility shows a major decrease at about 580 °C indicating the presence of magnetite (Fig. 3). An initial small increase in magnetic susceptibility up to ~300 °C can be due to several reasons: progressive unblocking of fine single-domain particles and their transition to the superparamagnetic state with increasing temperature [20]; or dehydration of iron hydroxides, such as lepidocrocite and goethite, followed by the formation of maghemite and/or hematite, respectively [21]. The steady decrease after 300 °C in the heating curves is generally interpreted as the conversion of metastable maghemite to weakly magnetic hematite [20]. Heating curves for the samples from pedocomplexes 9 and 10 do not detect hematite, while the loess sample shows a slight but noticeable decrease of magnetic susceptibility up to 700 °C which may indicate hematite. Magnetic susceptibility after cooling is 3–3.5 times higher, which is attributed to the neoformation of magnetite grains from paramagnetic minerals or Fe-containing silicates [22], or/and due to the formation of magnetite in a reducing atmosphere formed by the burning of organic matter [23] in the experimental tube.

Magnetic susceptibility values show an expected enhancement in soil horizons due to contribution of ultrafine ferrimagnetic minerals (magnetite, maghemite) formed by pedogenesis (Fig. 4). The data also show the monotonous nature of the material accumulation and its homogeneity in the loess interval. Pedocomplexes, and especially the LB horizon below the petrocalcic layer (Sca) of PC 9, are characterized by lower magnetic susceptibility values caused by abundant calcite developed along the roots in soils, or washed out of soil above, respectively.

The anisotropy of magnetic susceptibility data show that the minimum axes have steep nearly vertical directions shifted slightly to the southwest, while the maximum and intermediate axes are nearly horizontal and distributed around the great circle

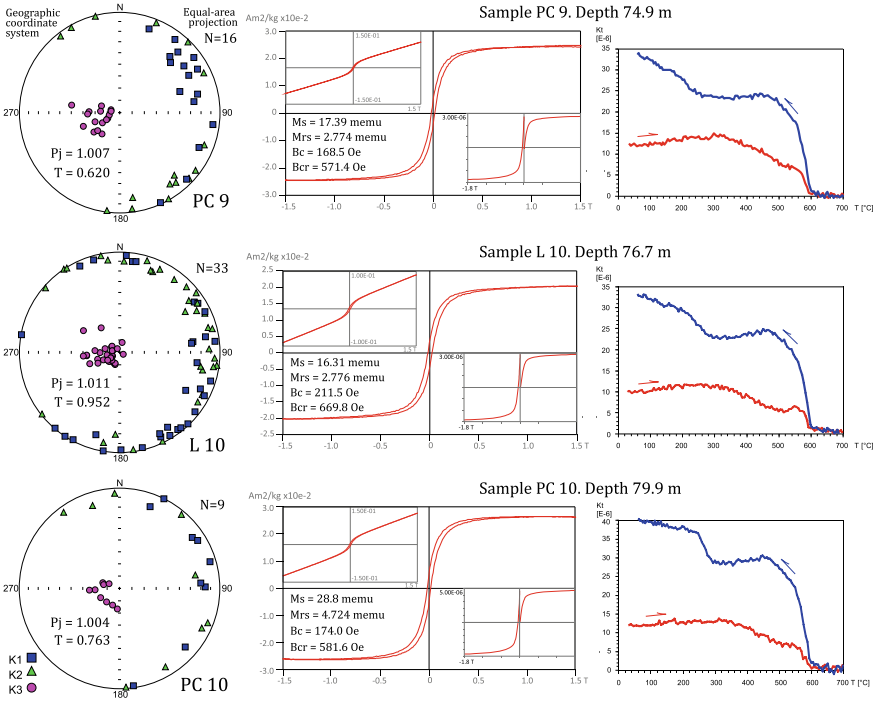

Fig. 3 Anisotropy of magnetic susceptibility, hysteresis loops, and temperature dependences of magnetic susceptibility for pedocomplexes 9 and 10 and loess 10. K1, K2, K3 are the maximum, intermediate, minimum axes of magnetic susceptibility, respectively. Hysteresis loops are mass normalized and corrected for dia-, paramagnetic contribution (raw loops are shown in insets). IRM acquisition and backfield demagnetization curves are also shown in insets. The red/blue curves in temperature dependence of magnetic susceptibility plots show heating/cooling

with certain prevailing directions in some cases (Fig. 3). Such southwestern displacement agrees with the direction of layers' dip dictated by the paleorelief surface. Therefore, the displacement of anisotropy axes is related to the peculiarities of the material accumulation. The data indicate the lack of strong disturbance of sediment structure that would produce a chaotic distribution of AMS axes.

3.2 Natural Remanent Magnetization

Representative orthogonal vector diagrams of the NRMs, stereograms and intensity demagnetization plots are shown in Fig. 5. The figure shows examples of diagrams for samples of normal polarity (a, b, c), intermediate (anomalous) (d, e, f), and reverse polarity (g, h, i). In general, samples have a good quality paleomagnetic

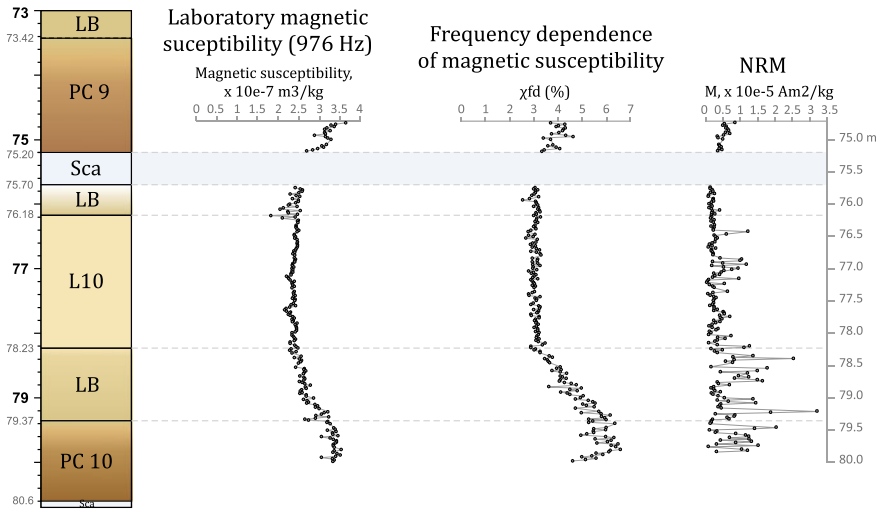

Fig. 4 Rock-magnetic parameters: laboratory magnetic susceptibility measured at 976 Hz, frequency dependence of magnetic susceptibility, and intensity of natural remanent magnetization (NRM). PC—pedocomplex, Sca—petrocalcic horizon, L—loess, LB—loess with pedogenic processes

record. The performance of the thermal demagnetization is generally better than that of alternating field (compare e.g. diagrams (a)/(b) and (h)/(i) in Fig. 5).

Samples mainly contain two magnetization components: (1) low-coercivity/low-temperature secondary component probably of viscous nature, (2) high-coercivity/high-temperature, presumably primary component of detrital/pedogenic nature, which we consider as characteristic (ChRM). The characteristic component typically starts unblocking at temperatures of 300 °C or alternating fields of 15–30 mT, respectively, and decays towards the origin. Initial NRM intensity is demagnetized by 90% on average. For samples from the transition zone, paleomagnetic record sometimes becomes noisy at high fields above 90 mT, and points on stereograms start to wander erratically (e.g. Fig. 5e).

3.3 Paleomagnetic Directions

Paleomagnetic directions (declination and inclination) for 230 stratigraphic levels, averaged over specimens from one level, are shown in Fig. 6. VGP latitudes calculated from characteristic NRM components (Fig. 6e) allowed distinguishing seven rapid flips of polarity (Fig. 6e) within a 2.89 m thick zone (depths 74.97–77.86 m). In most cases, the polarity transitions occur through intermediate VGP latitudes. Some of normal and reverse polarity subzones show stable remanence directions and have thickness of tens of centimeters, such as n1, r2 and n2. Multiple rapid polarity flips

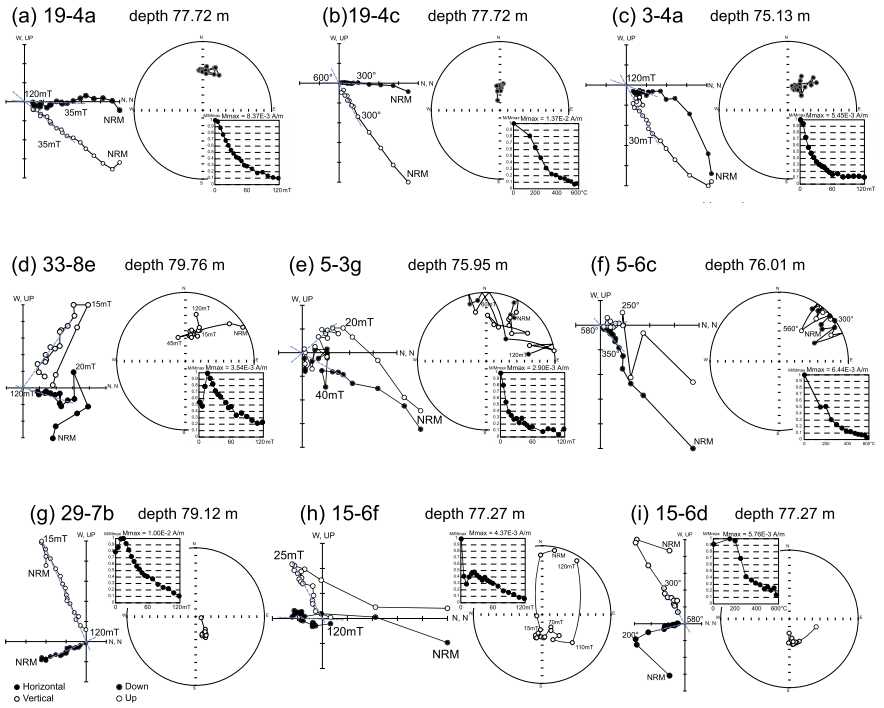

Fig. 5 Representative orthogonal vector diagrams of progressive thermal and alternating field demagnetization of natural remanent magnetization (NRM), stereograms of component direction, and intensity demagnetization plots for normal polarity samples (**a–c**), samples with anomalous directions (**d–f**) and reversed polarity samples (**g–i**). Stereograms are given in stratigraphic system

during Matuyama-Brunhes transition are a well-known feature found in many high-resolution loess records, as well as in marine, lacustrine, and volcanic sequences [24 and references therein]. The number of flips is different in various geological archives, so distant sites are difficult to correlate. The true nature of these flips remains unclear and may be either a real record of the geomagnetic reversal or the result of distortion of the paleomagnetic record due for example to lock-in effect, pedogenic, illuvial or bioturbation processes.

The stability of the paleomagnetic signal record is reflected by the mean value of MAD (Fig. 6c). The higher the MAD value, the lower the quality of the paleomagnetic record in the specimens and/or the lower the degree of clustering of specimen directions from one level. Such behavior is more likely a direct consequence of weak magnetic field intensity that always accompanies reversals and leads to poor magnetic alignment. Paleomagnetic record instability is seen in the entire zone of polarity flips. Particular attention should be paid to the zone of anomalous (and scattered at specimen level) directions in the lower part of the section with predominant stable reversed polarity. This zone, named $r1_a$, encompasses 22 cm (depths 79.76–79.98 m) and may record an excursion event in late Matuyama Chron (Fig. 6f).

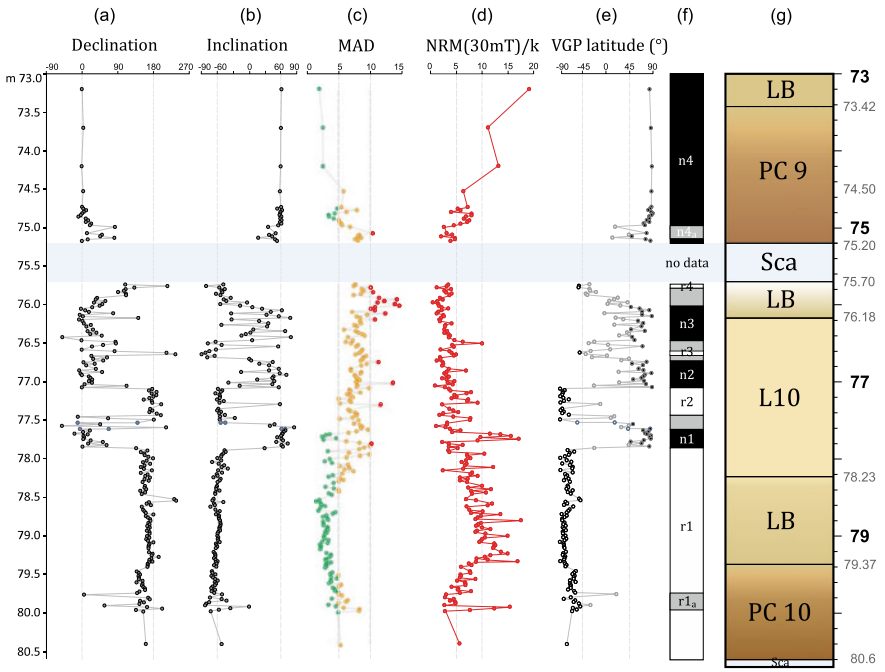

Fig. 6 Results of paleomagnetic studies of Kuldara site. **a**, **b** declination and inclination of the averaged component from every level. **c** median absolute deviation (MAD) averaged over samples from one level with the 5° and 10° cut-off limits (green circles correspond to MAD <5°, yellow circles—5–10°, red circles >10°). **d** intensity of NRM after demagnetization at 30 mT normalized by magnetic susceptibility. **e** latitude of VGP calculated from the component direction. **f** resulting polarity scale. **g** lithological chart

The behavior of the MAD values is consistent with and supported by data on intensity of $NRM_{(30\ mT)}$ normalized by magnetic susceptibility which serves as a rough proxy for relative paleointensity [25]. The lowest $NRM_{(30mT)}$/k values correspond to the transition zone and to the lower part of the studied interval in PC 10, $r1_a$ zone (Fig. 6d).

Another significant result is the presence of anomalous directions zone at the base of pedocomplex 9 (zone $n4_a$) and reversed polarity zone in the LB horizon immediately below the petrocalcic horizon (zone r4). This indicates the continuing instability of geomagnetic field and the completion of the M/B reversal already during interglacial of MIS 19.

4 Discussion

One of the most important issues is assessing the duration of the Matuyama-Brunhes transition in the Kuldara section. We made a rough age estimate based on correlation of lithological chart and magnetic susceptibility curve (Fig. 7b, c) with MIS sequence (Fig. 7d), and calculated the respective sedimentation rates. The loess-paleosol series of Tajikistan are very sensitive to climate change and reflect global climatic fluctuations in temperature and precipitation in many lithological features, such as thickness of loess layers between paleosols, soil type and its structure and degree of maturity, thickness of petrocalcic horizons. In turn, rock magnetic parameters, and primarily magnetic susceptibility, are sensitive to pedogenic processes that occurred through time in Tajikistan (even very poorly in epochs of loess accumulation, personal communication of P.M. Sosin, Institute of Water Problems, Hydroenergy and Ecology NAST, Dushanbe). Magnetic susceptibility curve allows to trace even minor changes in lithology. Therefore, our main tie-points for correlation were PC 9, PC 10 and L 10/LB boundaries. With support of magnetic susceptibility data, PC 9 was tentatively correlated to MIS 19c, L 10—to the cold stage MIS 20, LB and PC 10—to MIS 21.

Under these assumptions, the Matuyama-Brunhes transition in the Kuldara site would have a duration of ~22 kyr (809–787 ka). This age estimate is considerably older than published data from other sedimentary records [24, 26] and currently accepted age of the M/B boundary ~773 ka [27], indicating downward shift of the boundary in the studied section. In this case, the position of the last zone of reverse polarity—r4 zone in Figs. 6 and 7 —is especially important. The underlying normal polarity zones can be either a real reflection of the geomagnetic field behavior during the reversal, or an artifact of superimposed chemical remanent magnetization of younger age, as suggested in [28]. Multiple polarity flips observed in our section require further study. Comparison of Kuldara results with records of the M/B transition in other loess-paleosol sections in the same region and identification of common patterns or differences in the paleomagnetic signal would help to clarify this issue.

Excursion event ($r1_a$ zone in Figs. 6 and 7) is found in PC 10 which corresponds to MIS 21. According to our preliminary correlation, the excursion lasted ~5 kyr (852–847 ka) and occurred ~38 kyr prior to the beginning of polarity flips zone. Excursions are well known for late Matuyama Chron, the most common and recorded worldwide in lava flows [31, 32] and Chinese loess [33] being Kamikatsura and Santa Rosa events. The age of these events is mostly based on $^{40}Ar/^{39}Ar$ ages of lava flows, but is still not unified and is subject to revision and calibration. Kamikatsura event occurred 886 ± 3 ka according to [31], subsequently revised to 900.4 ± 4.6 ka [32]. The Santa Rosa excursion has been recorded in volcanic rocks from Tahiti, Hawaii, New Mexico, and Galapagos and has mean radioisotopic age of 927 ± 2 ka [31, 34]. Our excursion event, correlated to MIS 21, is younger than these two worldwide events, but is in good agreement with less well documented and still uncertain Takatsuki event [35] found at a higher stratigraphic level than the Kamikatsura event in marine sediments of the Osaka Group, Japan. The Takatsuki

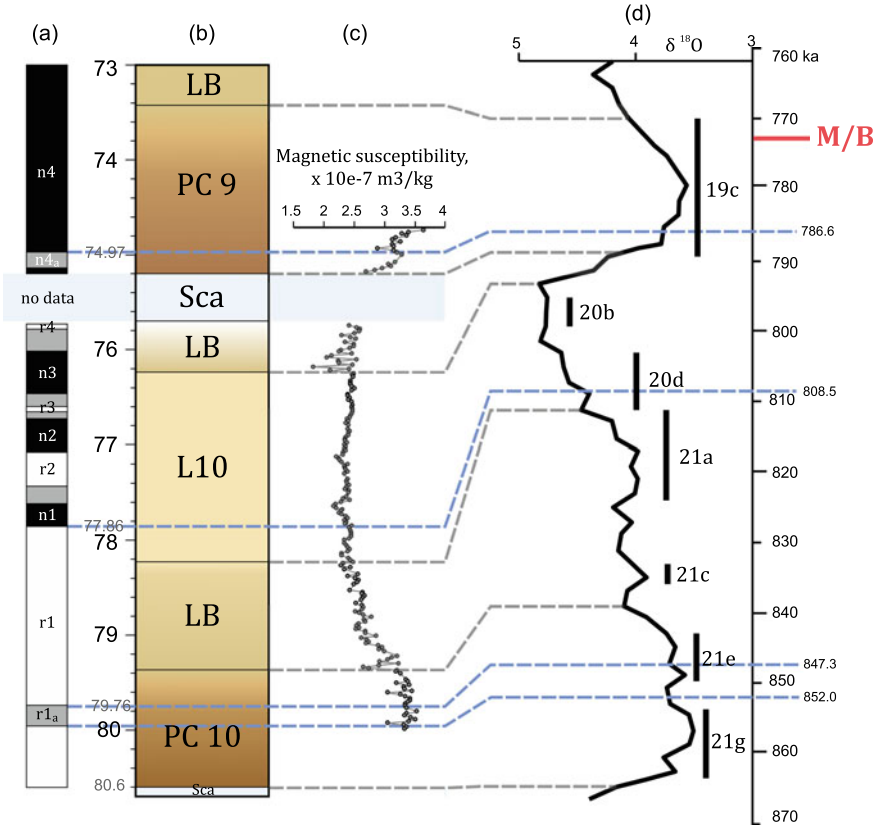

Fig. 7 Correlation of the studied interval of the Kuldara loess-paleosol sequence with MIS for preliminary age estimation. **a** resulting polarity scale. **b** lithological chart. **c** magnetic susceptibility. **d** benthic marine $\delta^{18}O$ record [29]. Position of the M/B boundary on the right age scale is given after [30]

excursion is found just above the Azuki tuff dated at 850 ± 30 ka [35] and should therefore have a close age.

VGP spatial distribution received from the Kuldara site is shown in Fig. 8. 38 VGPs were calculated from levels having highly scattered level-mean paleomagnetic directions with $\alpha_{95} > 45°$ (Fig. 8a, red circles). Such a large α_{95} is not related to the quality of determining the direction in each individual specimen, but rather results from averaging of specimens from the same level having highly discordant directions. The low degree of magnetic alignment is associated with a weak dipole field and therefore a paleomagnetic direction may be recorded with a large error. Since a VGP reflects the position of the magnetic South pole of a geocentric dipole, the calculation of VGP for such levels is not an adequate description of the transitional field. In the Fig. 8b, the VGPs with large α_{95}'s are not plotted.

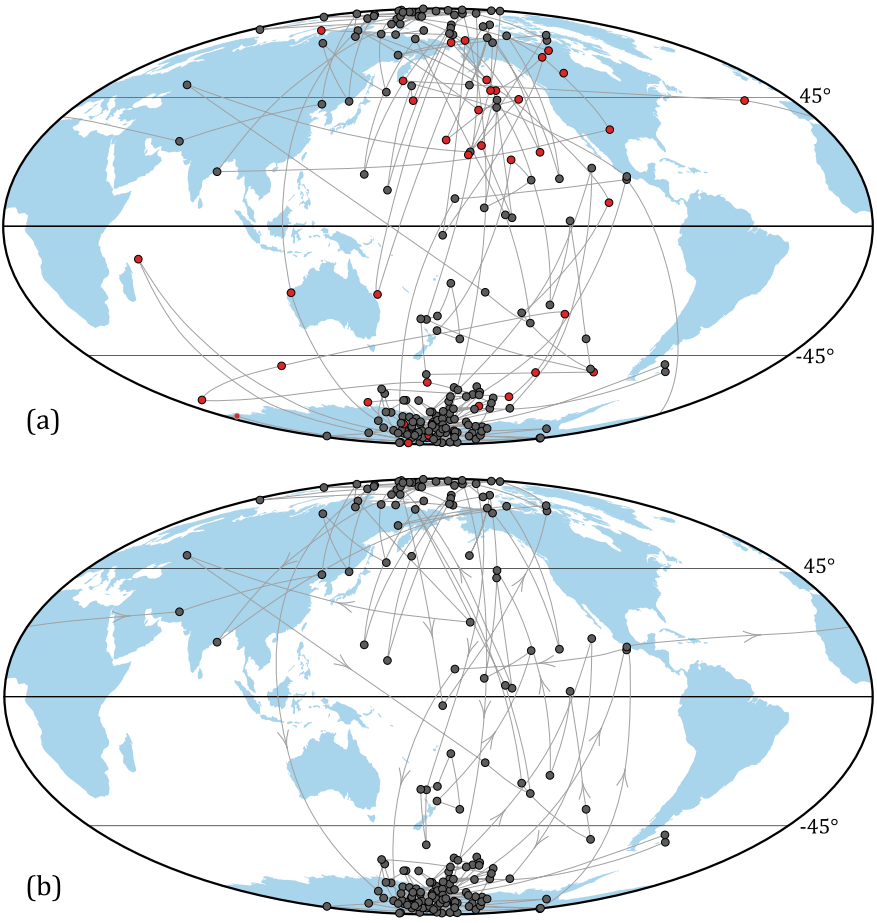

Fig. 8 VGP paths. **a** all data. **b** VGPs calculated from directions with $\alpha_{95} < 45$ (black circles). VGPs for levels with $\alpha_{95} > 45$ are shown with red circles

We have obtained 46 intermediate VGPs (−45° < VGP lat. <45°) due to high resolution of sampling including 16 VGPs with large α95. Most intermediate VGPs are concentrated in the Pacific longitudinal sector and just a few are scattered over Eurasia and North America. In the early 1990s, based on the collection of sedimentary M/B transition records, it has been observed that VGP paths have a longitudinal preference. Two preferred longitudinal bands have been distinguished—along the Americas and across East Asia [36]. However, detailed paleomagnetic directional data of M/B transition from other locations acquired later did not always support these preferred paths [37]. Leonhardt and Fabian [38] have tested the significance of preferred VGP paths by calculating the predicted paths for 642 equally distributed sites on the globe and found the Pacific hemisphere preference for transitional VGPs. It has also been established that dominance of non-dipolar components during the

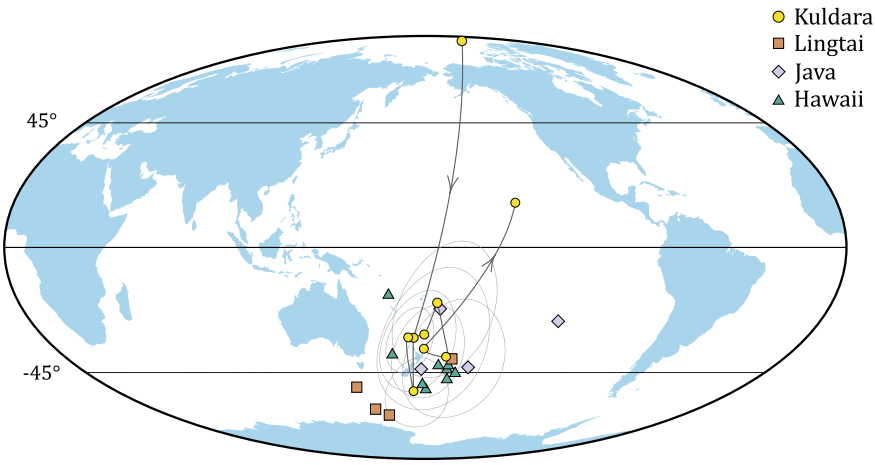

Fig. 9 Matuyama-Brunhes transitional VGPs clustered in the southwest Pacific: Kuldara loess site, Tajikistan (this study) with confidence ovals; Lingtai loess site, China [24]; Java lacustrine clays/silty clays site [39]; Hawaii lava flows site [32]

transition and the thermal structure of the lowermost mantle influence on the surface field record of intensity, declination and inclination make these characteristics (and VGP path longitudinal preference accordingly) site dependent.

Transitional VGPs from the Kuldara site are quite scattered except for a cluster in the SW Pacific region (Fig. 9), corresponding to the upper part of transitional M/B zone in the section (depths 75.74–75.88 m, approximate duration is ~600 yr). Similar SW Pacific cluster of transitional VGPs is known for loess-paleosol Lingtai section in the Chinese Loess Plateau [24], lacustrine clays of Java [39], and lava flows in the Haleakala section of Maui Island, Hawaii [32] (Fig. 9). For all of them these transitional VGPs also correspond to the upper part of the M/B transition record. In the Iterative Bayesian reversal model of Leonhardt and Fabian [38], regionally constrained VGP accumulations or VGP clusters are observed as well, and associated with local non-dipolar field directions and intensities at the Earth's surface caused by magnetic flux patches. These VGP clusters, which indicate time intervals of relatively stable local field directions, are mostly formed either between 778 and 776 kyr, or between 775 and 772 kyr, and last 1–2 kyr [38]. The first age interval (776–778 kyr) is in good agreement with the age estimations for horizons with SW Pacific clustered VGPs—the Ar–Ar ages of the Hawaiian lava flows [32] and the stratigraphic age estimates of the lacustrine clays of Java [39] and the loesses of the Lingtai section [24]. Our estimate of the M/B transition timing at the Kuldara site appears considerably older than commonly accepted ages, and requires further revision and additional studies on the magnetization formation mechanism. However, the transitional SW Pacific clustered VGPs and the comparability of our paleomagnetic record with other terrestrial archives may indicate that our record reflects the true behavior of

the geomagnetic field. The interval corresponding to these SW Pacific transitional VGPs may potentially be used as a tie-point for future refining age models.

5 Conclusion

We performed detailed a high-resolution paleomagnetic analysis of the Matuyama-Brunhes magnetic polarity transition in the loess-paleosol sequences at Kuldara site in southern Tajikistan. For the first time in the region, the end of the M/B reversal is reliably fixed at the beginning of warm climatic stage corresponding to MIS 19 and pedocomplex 9 of regional stratigraphy. The M/B polarity transition itself encompasses a ~ 3-m thick zone and includes both seven polarity flips and anomalous/intermediate directions. Its duration can be roughly estimated at 22 kyr (809–787 ka) showing a downward shift compared to the conventional age ~773 ka for the terminal M/B transition. We also found an excursion in late Matuyama Chron between 852–847 ka, ~38 thousand years prior to the reversal which occurs in a 22-cm thick zone with anomalous directions and instability of paleomagnetic signal.

M/B transition in Kuldara loess appears considerably older compared to other sedimentary and volcanic records. Magnetization acquisition in the studied loess therefore must have occurred with a delay, or the primary paleomagnetic signal was disturbed and/or rewritten by superimposed magnetization of younger age. A deeper study of the lithological features, age and rock magnetic properties of each horizon is necessary to better constrain the nature of the paleomagnetic record.

Acknowledgements We would like thank Donish Institute of history, archaeology and ethnography NAST, Dushanbe, for opportunity to work at Tajik loess palaeolithic site Kuldara. We acknowledge P.M. Sosin for fruitful discussion of regional loess stratigraphy during field works and lithological description of the section. This paper was greatly improved by thorough and constructive comments from two anonymous reviewers and editor Andrei Kosterov.

Funding This work is carried out within the state assignment of Schmidt IPE RAS and supported by the Russian Science Foundation under grant 22–18-00568.

References

1. Merrill, R. T., McFadden, P. L.: Geomagnetic polarity transitions. Reviews of Geophysics 37, 201–226 (1999).
2. Valet, J.-P., Fournier, A.: Deciphering records of geomagnetic reversals. Reviews of Geophysics 54(2), 410–446 (2016).
3. Li, Y., Shi, W., Aydin, A., Beroya-Eitner, M.A., Gao, G.: Loess genesis and worldwide distribution. Earth-Science Reviews 201, 102947 (2020).
4. Dodonov, A.E., Baiguzina, L.L.: Loess stratigraphy of Central Asia: Palaeoclimatic and palaeoenvironmental aspects. Quaternary Science Reviews 14(7-8), 707–720 (1995).
5. Muhs, D.R.: Loess and its geomorphic, stratigraphic and paleoclimatic significance in the Quaternary. Treatise on Geomorphology 11, 149–183 (2013).

6. Shackleton, N.J., An, Z., Dodonov, A.E., Gavin, J., Kukla, G.J., Ranov, V.A., Zhou, L.P.: Accumulation rate of loess in Tadjikistanand China: Relationship with global ice volume cycles. Quaternary Proceedings 4, 1–6 (1995).
7. Channell, J.E.T., Hodell, D.A., Singer, B.S., Xuan, C.: Reconciling astrochronological and $^{40}Ar/^{39}Ar$ ages for the Matuyama-Brunhes boundary and late Matuyama chron. Geochemistry, Geophysics, Geosystems 11, Q0AA12 (2010).
8. Zhou, L.P., Shackleton, N.J.: Misleading positions of geomagnetic reversal boundaries in Eurasian loess and implications for correlation between continental and marine sedimentary sequences. Earth and Planetary Science Letters 168(1-2), 117–130 (1999).
9. Dodonov, A.E., Shackleton, N.J., Zhou, L.P., Lomov, S.P., Finaev, A.F.: Geochronology, correlation, and evolution of paleoenvironments. Stratigraphy and Geological Correlation 7(6), 66–80 (1999).
10. Liu, Q., Jin, C., Hu, P., Jiang, Z., Ge, K., Roberts, A.P.: Magnetostratigraphy of Chinese loess-paleosol sequences. Earth-Science Reviews 150, 139–167 (2015).
11. Zhou, W., Beck, J.W., Kong, X., An, Z., Qiang, X., Wu, Z., Xian, F., Ao, H.: Timing of the Brunhes-Matuyama magnetic polarity reversal in Chinese loess using ^{10}Be. Geology 42(6), 467–470 (2014).
12. Dodonov, A.E., Pen'kov, A.V.: Some data on the stratigraphy of the watershed loesses in Tajik Depression. Bulletin of the Commisition on the Quaternary Research 47, 67–76 (1977). (in Russian)
13. Forster, Th., Heller, F.: Loess deposits from the Tajik depression (Central Asia): Magnetic properties and paleoclimate. Earth and Planetary Science Letters 128, 501–512 (1994).
14. Dodonov, A.E., Sadchikova, T.A., Sedov, S.N., Simakova, A.N., Zhou, L.P.: Multidisciplinary approach for paleoenvironmental reconstruction in loess-paleosol studies of the Darai Kalon section, Southern Tajikistan. Quaternary International 48–58, 152–153 (2006).
15. Dodonov, A.E.: Quaternary of Middle Asia. Stratigraphy, correlation, paleogeography. GEOS, Moscow, 250 p. (2002). (in Russian)
16. Ranov, V.A.: The 'loessic palaeolithic' in South Tadjikistan, Central Asia: Its industries, chronology and correlation. Quaternary Science Reviews 14(7-8), 731–745 (1995).
17. Kirschvink, J.L.: The least-squares line and plane and the analysis of paleomagnetic data. Geophysical Journal International 62(3), 699–718 (1980).
18. Fisher, R.A.: Dispersion on a sphere. Proceedings of the Royal Society. A Mathematical Physical and Engineering Sciences 217(1130), 295–305 (1953).
19. Dearing, J.A., Dann, R.J.L., Hay, K., Lees, J.A., Loveland, P.J., Maher, B.A., O'Grady, K.: Frequency-dependent susceptibility measurements of environmental materials. Geophysical Journal International 124(1), 228–240 (1996).
20. Liu, Q., Deng, C., Yu, Y., Torrent, J., Jackson, M.J., Banerjee, S.K., Zhu, R.: Temperature dependence of magnetic susceptibility in an argon environment: Implications for pedogenesis of Chinese loess/palaeosols. Geophysical Journal International 161, 102–112 (2005).
21. Evans, M.E., Heller, F.: Environmental Magnetism – Principles and Applications of Enviromagnetics. Academic Press, 293 p. (2003).
22. Hunt, C.P., Banerjee, S.K., Han, J., Solheid, P.A., Oches, E., Sun, W., Liu, T.: Rock-magnetic proxies of climate change in the loess-palaeosol sequences of the western Loess Plateau of China. Geophysical Journal International 123(1), 232–244 (1995).
23. Jeleńska, M., Hasso-Agopsowicz, A., Kopcewicz, B.: Thermally induced transformation of magnetic minerals in soil based on rock magnetic study and Mössbauer analysis. Physics of the Earth and Planetary Interiors 179(3-4), 164–177 (2010)
24. Hyodo, M., Banjo, K., Yang, T., Katoh, S., Shi, M., Yasuda, Y., Fukuda, J., Miki, M., Bradák, B.: A centennial-resolution terrestrial climatostratigraphy and Matuyama– Brunhes transition record from a loess sequence in China. Progress in Earth and Planetary Science 7, 26 (2020)
25. Tric, E., Valet, J.-P., Tucholka, P., Paterne, M., Labeyrie, L., Guichard, F., Tauxe, L., Fontugne, M.: Paleointensity of the geomagnetic field during the last 80,000 years. Journal of Geophysical Research 97(B6), 9337–9351 (1992).

26. Haneda, Y., Okada, M., Suganuma Y., Kitamura, T.: A full sequence of the Matuyama-Brunhes geomagnetic reversal in the Chiba composite section, Central Japan. Progress in Earth and Planetary Science 7, 44 (2020).
27. Singer, B.S., Jicha, B.R., Mochizuki, N., Coe, R.S.: Synchronizing volcanic, sedimentary, and ice core records of Earth's last magnetic polarity reversal. Science Advances 5(8), eaaw4621 (2019).
28. Spassov, S., Heller, F., Evans, M.E., Yue, L.P., von Dobeneck, T.: A lock-in model for the complex Matuyama-Brunhes boundary record of the loess/palaeosol sequence at Lingtai (Central Chinese Loess Plateau). Geophysical Journal International 155, 350–366 (2003).
29. Lisiecki, L.E., Raymo, M.E.: A Pliocene-Pleistocene stack of 57 globally distributed benthic $\delta^{18}O$ records. Paleoceanography 20, PA1003 (2005).
30. Cohen, K.M., Gibbard, P.L.: Global chronostratigraphical correlation table for the last 2.7 million years, version 2019 QI-500. Quaternary International 500, 20–31 (2019).
31. Singer, B.S., Hoffman, K.A., Chauvin, A., Coe, R.S., Pringle, M.S.: Dating transitionally magnetized lavas of the late Matuyama Chron: toward a new $^{40}Ar/^{39}Ar$ timescale of reversals and events. Journal of Geophysical Research 104, 679–693 (1999).
32. Coe, R.S., Singer, B.S., Pringle, M.S., Zhao, X.: Matuyama-Brunhes reversal and Kamikatsura event on Maui: paleomagnetic directions, $^{40}Ar/^{39}Ar$ ages and implications. Earth and Planetary Science Letters 222, 667–684 (2004).
33. Yang, T., Hyodo, M., Yang, Z., Fu, J.: Evidence for the Kamikatsura and Santa Rosa excursions recorded in eolian deposits from the southern Chinese Loess Plateau. Journal of Geophysical Research 109, B12105 (2004).
34. Channell, J.E.T., Singer, B.S., Jicha, B.R.: Timing of Quaternary geomagnetic reversals and excursions in volcanic and sedimentary archives. Quaternary Science Reviews 228, 106114 (2020).
35. Takatsugi, K.O., Hyodo, M.: A geomagnetic excursion during the late Matuyama Chron, the Osaka Group, southwest Japan. Earth and Planetary Science Letters 136, 511–524 (1995).
36. Clement, B.M.: Geographical distribution of transitional VGPs: Evidence for non-zonal equatorial symmetry during the Matuyama-Brunhes geomagnetic reversal. Earth and Planetary Science Letters 104, 48–58 (1991).
37. Prévot, M., Camps, P.: Absence of preferred longitude sectors for poles from volcanic records of geomagnetic reversals. Nature 366, 53–57 (1993).
38. Leonhardt, R., Fabian, K.: Paleomagnetic reconstruction of the global geomagnetic field evolution during the Matuyama/Brunhes transition: Iterative Bayesian inversion and independent verification. Earth and Planetary Science Letters 253, 172–195 (2007).
39. Hyodo, M., Matsu'ura, S., Kamishima, Y., Kondo, M., Takeshita, Y., Kitaba, I., Danhara, T., Aziz, F., Kurniawan, I., Kumai, H.: High-resolution record of the Matuyama-Brunhes transition constrains the age of Javanese Homo erectus in the Sangiran dome, Indonesia. Proceedings of the National Academy of Sciences of the United States of America 108(49), 19563–19568 (2011).